

Monte Carlo Shell Model and Shape Phase Transitions in Exotic Nuclei

Takaharu Otsuka^{a,b,c}, Yusuke Tsunoda^a, Noritaka Shimizu^b,
Michio Honma^d and Yutaka Utsuno^e

^a*Department of Physics, the University of Tokyo, Hongo, Tokyo 113-0033, Japan*

^b*Center for Nuclear Study, the University of Tokyo, Hongo, Tokyo 113-0033, Japan*

^c*National Superconducting Cyclotron Laboratory, Michigan State University, East Lansing, MI 48824, USA*

^d*Center for Mathematical Sciences, University of Aizu, Ikkimachi, Aizu-Wakamatsu, Fukushima 965-8580, Japan*

^e*Advanced Science Research Center, Japan Atomic Energy Agency, Tokai, Ibaraki 319-1195, Japan*

Abstract

The shapes of neutron-rich exotic Ni isotopes are studied in terms of large-scale shell model calculations performed by advanced Monte Carlo Shell Model (MCSM) for the $pf\text{-}g_{9/2}\text{-}d_{5/2}$ model space. Experimental energy levels are reproduced well by a single fixed Hamiltonian based on A3DA. Intrinsic shapes are analyzed for MCSM eigenstates including fluctuations. Intriguing interplays among spherical, oblate, prolate and γ -unstable shapes are seen including shape fluctuations, $E(5)$ -like situation, the magicity of doubly-magic $^{56,68,78}\text{Ni}$, and the coexistence of spherical and strongly deformed shapes.

Keywords: Monte Carlo Shell Model; Ni isotopes; shape coexistence

1 James and us

It is a great pleasure for me to give this talk in the conference celebrating the 70th birthday of James P. Vary. James has given great supports not only to the development of Monte Carlo Shell Model by our group but also to computational nuclear physics activities in Japan. We are very much grateful to his efforts, enthusiasm and actual collaborations. In fact, the nuclear structure theory group in the University of Tokyo (Tokyo group) has enjoyed many collaborations with James and his colleagues in Ames. We visited Ames many times, while James and Pieter Maris visited Japan also many times. Figure 1 shows several of Japanese members with colleagues in Ames at one of such occasions on the 28th of February, 2010.

2 Introduction

The Monte Carlo Shell Model has been explained to a good detail by Abe with co-authors in this proceedings [1]. We then skip the description of the method, and discuss what have been and can be obtained. We further restrict ourselves to calculations for heavier nuclei such as Ni isotopes. The size of the calculation is quite huge, though. We start with the motivations of such studies.

Proceedings of International Conference ‘Nuclear Theory in the Supercomputing Era — 2013’ (NTSE-2013), Ames, IA, USA, May 13–17, 2013. Eds. A. M. Shirokov and A. I. Mazur. Pacific National University, Khabarovsk, Russia, 2014, p. 286.

<http://www.ntse-2013.khb.ru/Proc/Otsuka.pdf>.

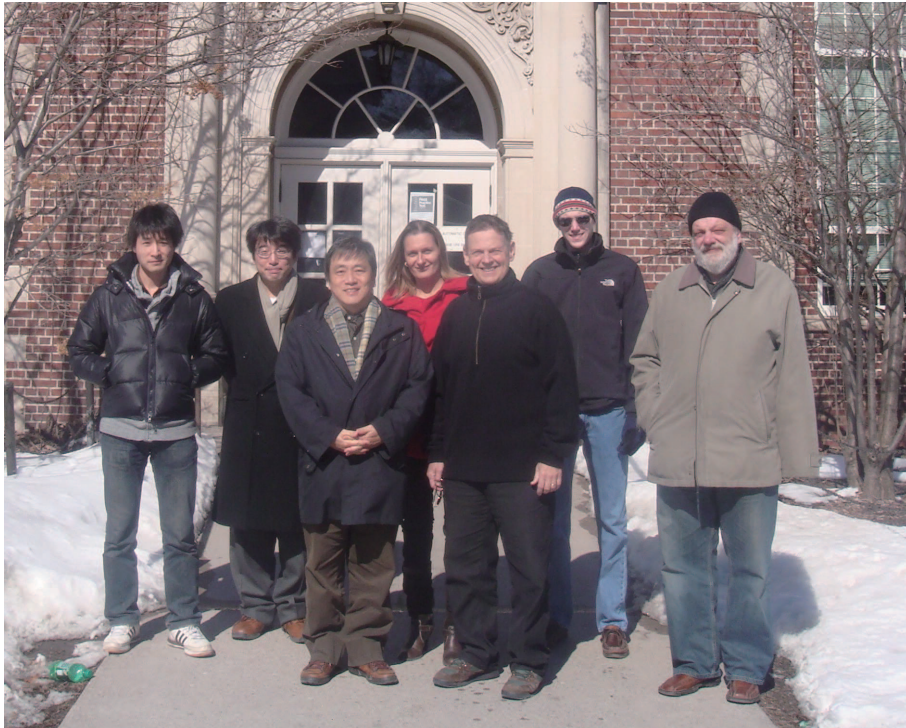


Figure 1: Photo taken in front of the Department of Physics, the Iowa State University on the 28th of February, 2010.

Atomic nuclei exhibit simple and robust regularities in their structure comprised of Z protons and N neutrons. A very early example is the (spherical) magic numbers conceived by Mayer and Jensen [2]. These magic numbers dominate low-energy dynamics of stable nuclei and their neighbors on the Segré chart. Another basic feature is nuclear shape, which has been one of the central issues of nuclear physics since Rainwater [3] and Bohr and Mottelson [4]. The shape varies as Z or N changes in such a way that it tends to be spherical near magic numbers, while becomes more deformed towards the middle of the shell. Thus, Z and N , in connection to the magic numbers, are known to be key variables in determining the shape of stable nuclei. Rare isotope beam technology developed since [5] has made experiments on exotic nuclei feasible, casting challenges to the pictures mentioned above. Even magic numbers are not exception: the changes of the shell structure due to nuclear forces, referred to as *shell evolution* [6], have been seen including disappearance of traditional magic numbers and appearance of new ones. A recent example is the discovery of $N = 34$ magic number [7] after its prediction a decade ago [8], while many other cases have been discussed [6, 9–11].

It is then of much interest to explore shapes of exotic nuclei and to look for relations to the shell evolution. In this talk, we report results of state-of-the-art large-scale shell model calculations for a wide range of Ni isotopes, focusing on these points. While the ground state turns out to be spherical basically, a strongly prolate deformed band appears at low excitation energy in some nuclei, similarly to shape coexistence known as a distinct phenomenon over decades [12–14]. The formation of this band is discussed in relation to reduced shell gaps brought about by the proton-neutron tensor force in major configurations (of single-particle orbits) of deformed states. (We introduced, after the conference, a new type of shell evolution due to configuration changes within the same nucleus, calling it *Type II shell evolution*. The shell evolution by the change of N or Z [6] is then referred to as *Type I*.) We shall

discuss other interesting features, e. g., magicity of doubly-magic $^{56,68,78}\text{Ni}$, shape fluctuations including γ instability, and $E(5)$ -like case [15].

We discuss, in this talk, the structure of Ni isotopes with even $N = 28\text{--}50$, utilizing results obtained by the advanced Monte Carlo Shell Model (MCSM) calculation [16–18] run on K computer for $\sim 2 \times 10^{10}$ core seconds in total. The model space consists of the full pf shell, $0g_{9/2}$ and $1d_{5/2}$ orbits for both protons and neutrons. There is no truncation within this space as an advantage of MCSM. The Hamiltonian is based on the A3DA Hamiltonian with minor revisions [16, 19]. The spurious center-of-mass motion is removed by the Lawson method [20].

3 Results for Ni isotopes

Figure 2 shows yrast and yrare levels by the present calculation compared to experiment [21]. Systematic behaviors are visible in experimental yrast levels as well as $J^\pi = 0_2^+$ and 2_2^+ yrare levels, with a remarkable agreement to the theoretical trends. Such good agreement has been obtained with a single fixed Hamiltonian, and suggests that the structure of Ni isotopes can be studied with it. The $B(E2; 0_1^+ \rightarrow 2_1^+)$ values with neutron and proton effective charges, 0.5 and 1.5, respectively, are shown in Fig. 2 compared to experiment [23] with certain discrepancies for heavier isotopes,

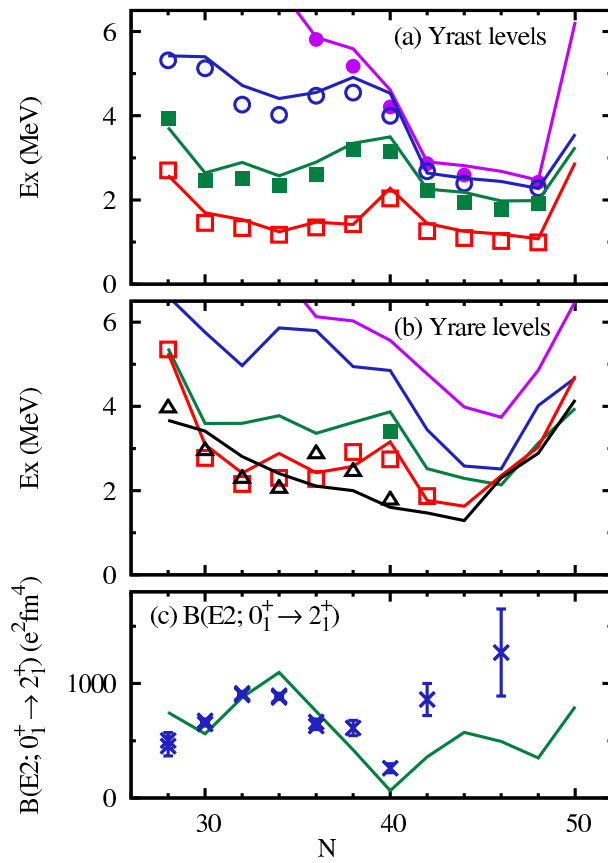


Figure 2: Energy levels for (a) yrast and (b) yrare states of Ni isotopes with even N . Symbols are experimental data for $J^\pi=0^+$ (black triangle), 2^+ (open red square), 4^+ (green filled square), 6^+ (open blue circle) and 8^+ (filled purple circle) [21, 22]. Lines are present MCSM calculations with the same color code. (c) $B(E2; 0_1^+ \rightarrow 2_1^+)$ values by experiment [23] and by the present calculation.

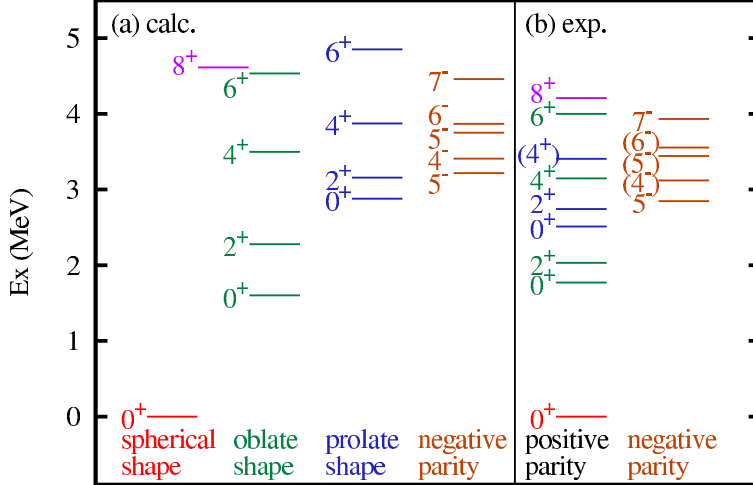


Figure 3: Energy levels of ^{68}Ni by present calculation (left panel) and by experiment (right panel) [21].

where uncertainties are larger and (p, p') data is converted ($N = 46$) [24, 25]. A more systematic comparison with precise data is desired. Relevant shell model calculations have been reported [26, 27]. In particular, those of [26] are remarkable achievement of large-scale conventional shell-model approach, with good agreement to experiment. Many experimental data are, however, to be obtained, and it is not the purpose of this work to compare different calculations. The primary objective here is to predict novel systematic change of band structures in $^{68-78}\text{Ni}$ isotopes.

We show, in Fig. 3, a more detailed level scheme for ^{68}Ni , including negative-parity states. This nucleus has attracted much attention [22, 27–34] from theoretical and experimental sides. The positive-parity levels are classified according to their shape categories: spherical, oblate and prolate. We shall come to this point later. The correspondence between theoretical and experimental levels can be made with rather good agreement. Note that this is the first report of calculated levels beyond 2^+ and those of negative-parity.

4 Intrinsic shapes and wave functions

Figure 4 depicts, for selected states of $^{68,70,74,78}\text{Ni}$ isotopes, potential energy surface (PES) for the present Hamiltonian obtained by the Constraint Hartree–Fock (CHF) method with usual constraints on quadrupole moments Q_0 and Q_2 . We can see many features: for instance, for ^{68}Ni , there is a spherical minimum stretched towards modest oblate region, as well as a prolate local minimum.

The MCSM wave function is expressed by a superposition of Slater determinants with the angular-momentum and parity projector $P[J^\pi]$,

$$\Psi = \sum_i c_i P[J^\pi] \Phi_i. \quad (1)$$

Here, c_i denotes an amplitude, Φ_i stands for the Slater determinant consisting of one-nucleon wave functions $\phi_1^{(i)}, \phi_2^{(i)}, \dots, \phi_n^{(i)}$ with

$$\phi_k^{(i)} = \sum_l D_{k,l}^{(i)} u_l, \quad (2)$$

where u_l is the l -th single-particle state in the original model space in m -scheme,

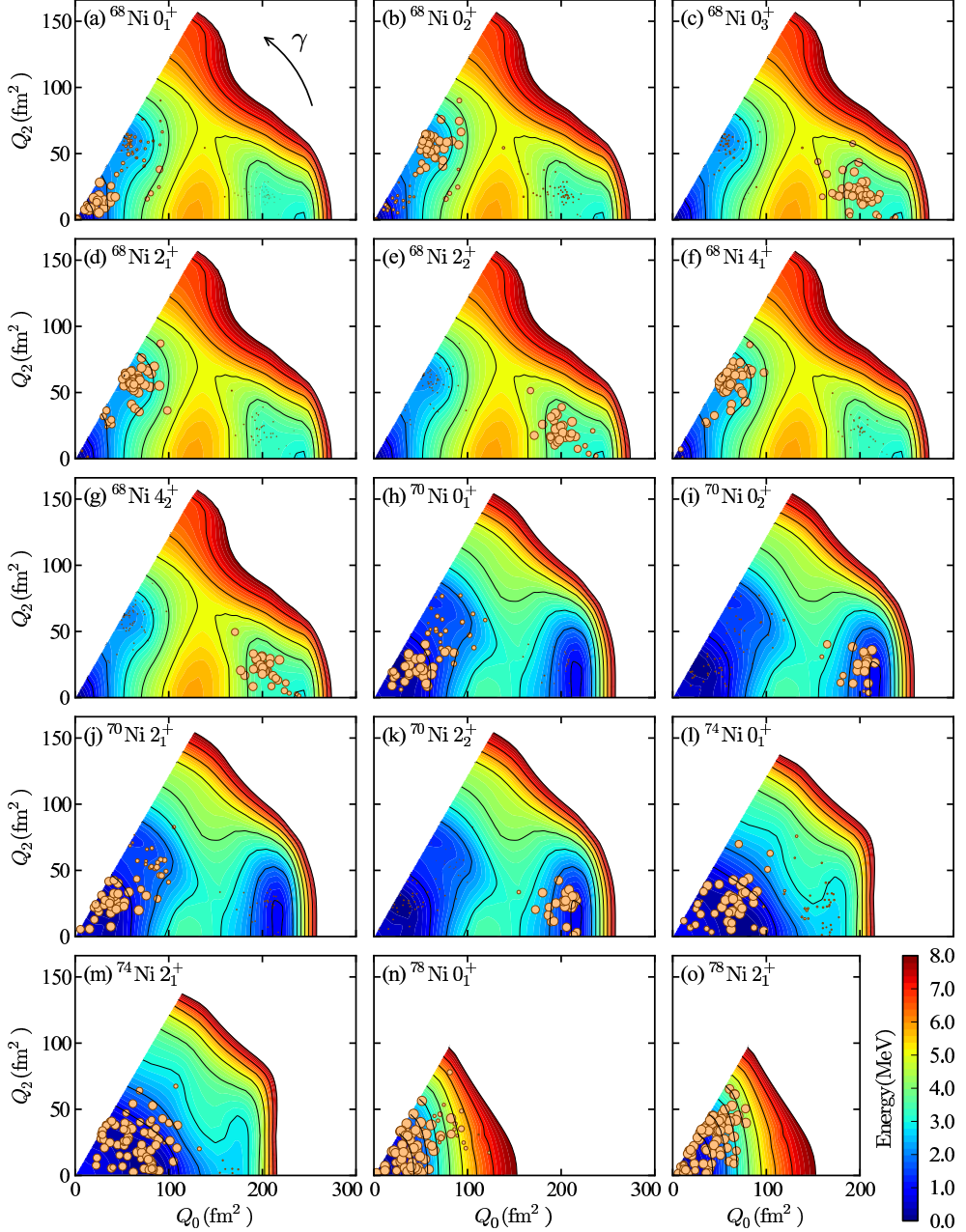


Figure 4: Potential energy surfaces (PES) of Ni isotopes, coordinated by usual Q_0 and Q_2 (or γ). The energy relative to the minimum is shown by contour plots. Circles on the PES represent shapes of MCSM basis vectors (see the text).

and D implies amplitude determined by MCSM process. Φ_i is the product of proton and neutron sectors, with n being the number of valence protons or neutrons.

For each Φ_i , we take the following process. We calculate its quadrupole moment matrix, and diagonalize. Three axes are obtained with Q_0 and Q_2 values. We then place a circle on the PES at the point corresponding to these Q_0 and Q_2 values. The size (i.e. area) of the circle is set to be proportional to the overlap probability between Ψ and the normalized $P[J^\pi] \Phi_i$. Thus, the location of the circle implies the intrinsic shape of Φ_i , and its size the importance of it in the eigenstate, Ψ . Note

that the states $P[J^\pi]\Phi_i$ ($i = 1, 2, \dots$) are not orthogonal each other in general, but the distribution pattern of the circles provides unique and clear message on intrinsic shape of the shell-model eigenstate as we shall see.

Figure 4(a) shows such circles for the ground state of ^{68}Ni . We see many large circles near the spherical point, $Q_0 = Q_2 = 0$. In general, there can be many points close to one another partly because each circle represents a Slater determinant and a two-body interaction, particularly its pairing components, mixes different Slater determinants. Those Slater determinants should have similar shapes so that the mixing between them can occur. We see also notable spreading of circle distribution from the spherical point. This implies the extent of the shape fluctuation. The 0_2^+ state in Fig. 4(b) shows similar spreading but the locations are shifted to moderately oblate region ($\beta_2 \sim -0.2$). Although there is no clear potential barrier between the spherical and oblate regions of the PES, the antisymmetrization pushes the 0_2^+ state away from the 0_1^+ state. Figure 4(c) exhibits many circles in a profound prolate minimum with $Q_0 \sim 200 \text{ fm}^2$ ($\beta_2 \sim 0.4$). We emphasize that we can analyze, in this way, the intrinsic shape even for 0^+ states without referring to E2 properties.

Figures 4(d, e) show the same plots for the $2_{1,2}^+$ states, while Figs. 4(f, g) the same plots for the $4_{1,2}^+$ states. The 2_1^+ and 4_1^+ states exhibit patterns almost identical to that of the 0_2^+ state, which suggests the formation of the modestly-oblate band. We would like to emphasize that the present analysis is very useful to identify the band structure buried in many-body calculations. Such striking similarity is found also among the 0_3^+ , 2_2^+ and 4_2^+ states with a strong-prolate-band assignment. We mention that a band similar to this prolate band has been pointed out by a shell-model calculation in [33]. The band structure is thus clarified, with further verification by $E2$ matrix elements, and is presented in Fig. 3 including 4^+ and 6^+ members.

The prolate band being discussed comes down to the 0_2^+ and 2_2^+ states as N increases from 40 to 42 or 44 [see Figs. 4(h, k)]. Observed 2_2^+ level of ^{70}Ni is as low as 2 MeV, which is reproduced well by the present calculation as shown in Fig. 2(b), whereas this level has not been reproduced by calculations with limited configurations [35, 36]. In addition, Fig. 2(a) depicts the 2_1^+ levels in good agreement to experiment, while strong fluctuation is seen towards oblate shape in Figs. 4(h, k). This work is the first report from theory for this low-lying 2_2^+ state.

In moving to ^{74}Ni , Figs. 4(l, m) exhibit another interesting pattern. The distribution of the circles becomes wide in both magnitude and γ direction, i. e., triaxiality. A similar distribution is obtained also for the 2_2^+ states, and the situation is the same for ^{76}Ni . It is of interest that this resembles the critical point symmetry $E(5)$ [15].

Finally, we come to ^{78}Ni . This is supposed to be a doubly closed shell nucleus. Figures 4(n, o) show the PES and wave function distribution for the 0_1^+ and 2_1^+ states. The PES goes up rapidly, but to be surprising, the wave functions are spread on the bottom fully, in a almost identical ways between the 0_1^+ and 2_1^+ states, which clearly differs from what we can expect from a closed shell. The distribution is much wider than that of ^{68}Ni . It is of much interest that comparing to ^{56}Ni and ^{78}Ni , ^{68}Ni is the closest to the doubly closed picture among the three doubly magic isotopes of Ni.

5 Summary

In summary, the advanced MCSM calculations present intriguing variations of shapes analyzed in terms of intrinsic shapes. Thus, the shapes of exotic nuclei provide us with many new features. In stable nuclei, the shape has been often discussed as functions of N and Z , for instance, shape evolution from vibrational to rotational nuclei as N increases. Such simple classification may no longer be appropriate in exotic nuclei. The role of large-scale shell-model calculations is quite significant, and will become even more important in future.

Acknowledgments

This work was in part supported by MEXT Grant-in-Aid for Scientific Research (A) 20244022. This work has been supported by HPCI (hp120284 and hp130024), and is a part of the RIKEN-CNS joint research project on large-scale nuclear-structure calculations. Y.T. acknowledges JSPS for Research Fellow (No. 258994).

References

- [1] T. Abe, P. Maris, T. Otsuka, N. Shimizu, Y. Tsunoda, Y. Utsuno and J. P. Vary, *see these Proceedings*, p. 294, <http://www.ntse-2013.khb.ru/Proc/Abe.pdf>.
- [2] M. G. Mayer, Phys. Rev. **75**, 1969 (1949); O. Haxel, J. H. D. Jensen and H. E. Suess, Phys. Rev. **75**, 1766 (1949).
- [3] J. Rainwater, Phys. Rev. **79**, 432 (1950).
- [4] A. Bohr and B. R. Mottelson, *Nuclear Structure, vol. II*. Benjamin, Reading, Mass., 1975, and World Scientific, Singapore, 1998.
- [5] I. Tanihata *et al.*, Phys. Rev. Lett. **55**, 2676 (1985).
- [6] For a brief review see T. Otsuka, Phys. Scr. T **152**, 014007 (2013).
- [7] D. Stepenbeck *et al.*, Nature **502**, 207 (2013).
- [8] T. Otsuka *et al.*, Phys. Rev. Lett. **87**, 082502 (2001).
- [9] For reviews from experimental side see A. Gade and T. Glasmacher, Progr. Part. Nucl. Phys. **60**, 161 (2008); O. Sorlin and M.-G. Porquet, Progr. Part. Nucl. Phys. **61**, 602 (2008).
- [10] T. Otsuka *et al.*, Phys. Rev. Lett. **95**, 232502 (2005).
- [11] T. Otsuka *et al.*, Phys. Rev. Lett. **104**, 012501 (2010).
- [12] H. Morinaga, Phys. Rev. **101**, 254 (1956).
- [13] K. Heyde and J. L. Wood, Rev. Mod. Phys. **83**, 1467 (2011).
- [14] A. N. Andreyev *et al.*, Nature **405**, 430 (2000).
- [15] F. Iachello, Phys. Rev. Lett. **85**, 3580 (2000).
- [16] N. Shimizu, T. Abe, Y. Tsunoda, Y. Utsuno, T. Yoshida, T. Mizusaki, M. Honma and T. Otsuka, Progr. Theor. Exp. Phys. 01A205 (2012).
- [17] N. Shimizu, Y. Utsuno, T. Mizusaki, T. Otsuka, T. Abe and M. Honma, Phys. Rev. C **82**, 061305(R) (2010).
- [18] T. Otsuka, M. Honma, T. Mizusaki, N. Shimizu and Y. Utsuno, Progr. Part. Nucl. Phys. **47**, 319 (2001).
- [19] Details available upon request to the corresponding authors.
- [20] D. H. Gloeckner and R. D. Lawson, Phys. Lett. B **53**, 313 (1974).
- [21] Evaluated Nuclear Structure Data File (ENSDF),
<http://www.nndc.bnl.gov/ensdf/>.

- [22] R. Broda *et al.*, Phys. Rev. C **86**, 064312 (2012); R. Broda, B. Fornal, W. Królas, T. Pawłat, D. Bazzacco, S. Lunardi, C. Rossi-Alvarez, R. Menegazzo, G. de Angelis, P. Bednarczyk, J. Rico, D. De Acuna, P. J. Daly, R. H. Mayer, M. Sferrazza, H. Grawe, K. H. Maier and R. Schubart, Phys. Rev. Lett. **74**, 868 (1995).
- [23] B. Pritychenko, J. Choquette, M. Horoi, B. Karamy and B. Singh, At. Data Nucl. Data Tables **98**, 798 (2012).
- [24] O. Perru *et al.*, Phys. Rev. Lett. **96**, 232501 (2006).
- [25] N. Aoi *et al.*, Phys. Lett. B **692**, 302 (2010).
- [26] S. M. Lenzi, F. Nowacki, A. Poves and K. Sieja, Phys. Rev. C **82**, 054301 (2010); references therein.
- [27] K. Kaneko, M. Hasegawa, T. Mizusaki and Y. Sun, Phys. Rev. C **74**, 024321 (2006)
- [28] M. Girod, P. Dessagne, M. Bernas, M. Langevin, F. Pougeon and P. Roussel, Phys. Rev. C **37**, 2600 (1988).
- [29] T. Ishii *et al.*, Phys. Rev. Lett. **84**, 39 (2000).
- [30] O. Sorlin *et al.*, Phys. Rev. Lett. **88**, 092501 (2002).
- [31] K. Langanke, J. Terasaki, F. Nowacki, D. J. Dean and W. Nazarewicz, Phys. Rev. C **67**, 044314 (2003).
- [32] D. Pauwels, J. L. Wood, K. Heyde, M. Huyse, R. Julin and P. Van Duppen, Phys. Rev. C **82**, 027304 (2010).
- [33] A. Dijon *et al.*, Phys. Rev. C **85**, 031301(R) (2012).
- [34] C. J. Chiara *et al.*, Phys. Rev. C **86**, 041304(R) (2012).
- [35] M. Honma, T. Otsuka, T. Mizusaki and M. Hjorth-Jensen, Phys. Rev. C **80**, 064323 (2009).
- [36] B. Cheal *et al.*, Phys. Rev. Lett. **104**, 252502 (2010).